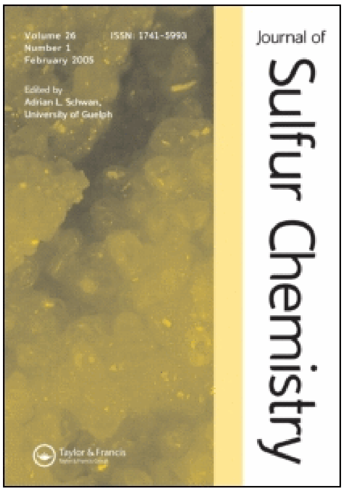

Journal of Sulfur Chemistry
Publication details, including instructions for authors and subscription information:
http://www.informaworld.com/smpp/title~content=t713926081

Decomposition and phase transition of NiS/Ni$_{1\text{-<i>x</i>}}$S in the temperature range 323-973 K

H. Wang[a]
[a] School of Chemical Engineering, University of Adelaide, Adelaide, SA, Australia

To cite this Article Wang, H.(2005) 'Decomposition and phase transition of NiS/Ni$_{1\text{-<i>x</i>}}$S in the temperature range 323-973 K', Journal of Sulfur Chemistry, 26: 3, 233 — 243
To link to this Article: DOI: 10.1080/17415990500195172
URL: http://dx.doi.org/10.1080/17415990500195172

Journal of Sulfur Chemistry
Vol. 26, No. 3, June 2005, 233–243

Taylor & Francis
Taylor & Francis Group

RESEARCH ARTICLE

Decomposition and phase transition of NiS/$Ni_{1-x}S$ in the temperature range 323–973 K

H. WANG*

School of Chemical Engineering, University of Adelaide, Adelaide, SA 5005, Australia

(Received 16 March 2005; in final form 25 May 2005)

Although the phase relations in the Ni–S system have been studied by many researchers, an accurate decomposition temperature range of the near equimolar composition α-NiS/α-$Ni_{1-x}S$ has not been established due to the complexity brought by the nonstoichiometic nature of α-NiS/α-$Ni_{1-x}S$. In the current study, a series of α-NiS/α-$Ni_{1-x}S$ synthetic schedules were adopted to study the phase relations and variations in cell parameters of various phases in the temperature range 323–643 K. The decomposition of NiS started above 773 K according to the reaction:

$$\alpha\text{-NiS} \longrightarrow \alpha\text{-Ni}_{1-x}\text{S} + (\text{Ni}_{3-x}\text{S}_2)$$

where $Ni_{3-x}S_2$ is high-temperature heazlewoodite. The Ni_3S_2 (low-temperature heazlewoodite) and a possible phase, Ni_7S_6, (the uncertainty is due to its low diffraction intensity in XRD profiles) observed in the current study are the products of the instantaneous decomposition of $Ni_{3-x}S_2$ during quenching from 973 K. The exsolutions of Ni_3S_2 and Ni_7S_6 during the quenching are less significant for compositions $Ni_{0.97}S$ and $Ni_{0.92}S$ compared with NiS.

For equimolar composition α-NiS, the exact transition temperature of α-NiS $\leftrightarrow$ β-NiS (millerite) lies between 623 K (derived from a cooling process) and 670 K (derived from a heating process). For nickel-deficient composition $Ni_{0.97}S$, α- and β-phases coexist in the temperature range 573–613 K, and the onset temperature for α- to β-phase transition is lowered by around 50 K (for cooling processes) compared with that of NiS.

Keywords: α-NiS; millerite; decomposition; phase relation

1. Introduction

The complete phase diagram of the Ni–S system was first introduced by Kullerud and Yund [1]. However, the relationship between the composition variations of the nonstoichiometic α-$Ni_{1-x}S$ and β-$Ni_{1-y}S$ and temperature in the near-equimolar (NiS) composition range have not been accurately solved, nor has the decomposition behavior of α-NiS/$Ni_{1-x}S$ upon heating.

The two well-studied forms of Ni(II) sulfide are β-NiS (millerite) and α-NiS. β-NiS, with a trigonal/rhombohedral crystal structure, is naturally formed as a low-temperature hydrothermal or alteration product of other nickel minerals. β-NiS is called millerite after W. H. Miller, the mineralogist who first studied millerite crystals [2]. Compared with α-NiS,

---

*Corresponding author. Email: haipeng.wang@adelaide.edu.au

Journal of Sulfur Chemistry
ISSN 1741-5993 print/ISSN 1741-6000 online © 2005 Taylor & Francis
http://www.tandf.co.uk/journals
DOI: 10.1080/17415990500195172

β-NiS is always referred to as the low-temperature form of NiS (<652 K), which has a high metallic conductivity and is speculated to possess a diamagnetic structure [3]. In Nature, millerite is more commonly found than is the α-phase, and it is of metallurgical interest, as millerite is often associated with other important nickel–iron or copper–iron ores [4–6]. Millerite generally occurs in fine hairlike or capillary crystals, thereby giving rise to the synonyms: "hair pyrite" and "capillary pyrite". β-NiS has near equimolar composition NiS, whereas α-NiS has a variable composition range, α-$Ni_{1-x}S$ [7]. The maximum x-value (as in α-$Ni_{1-x}S$) varies with temperature, and the relationship between x (as in α-$Ni_{1-x}S$) and temperature has not been precisely constructed [1, 7–9].

The high-temperature phase, α-NiS/α-$Ni_{1-x}S$, with a NiAs-type hexagonal structure, is quenchable and has been found as a metastable phase under ambient conditions. It has not been found in Nature as a mineral [8]. There have been numerous studies on this metastable α-NiS/α-$Ni_{1-x}S$ at low temperatures due to the distinct metal → semiconductor transition (MS transition) of α-NiS at 265 K, below which a small band gap occurs; this gap progressively increases with decreasing temperature [10–12]. α-NiS/α-$Ni_{1-x}S$ also plays an important role in studies of the crystal chemistry and phase relations in metal sulfides systems because of its relationship with other economically important Ni-bearing sulfide minerals, and especially because α-NiS and pyrrhotite are structurally related so that α-NiS may be considered to be a compositional Ni end-member of nickeliferous pyrrhotite, $(Ni,Fe)_{1-x}S$ [6, 13]. The NiAs-type structure of α-NiS exhibits a paramagnetic–antiferromagnetic transition at 265 K (Néel temperature). The sublattice magnetization goes from zero to full saturation on cooling through 265 K [6, 13].

Upon heating, the low-temperature stable phase β-NiS (millerite) transforms to the high-temperature form, α-NiS, at 652 K [1]. This transition temperature ($T_{\beta-\alpha}$) was measured at ambient pressure. Sowa *et al.* reported that $T_{\beta-\alpha}$ exhibits strong pressure dependence [14]. The temperature of the transition from millerite to NiAs-type NiS decreases drastically with increasing pressure. Owing to the higher compressibility of β-NiS (millerite) compared with that of the α-phase, the NiAs-type structure is believed to be unstable at high pressures. The number of the nearest sulfur atoms to a given nickel atom changes from 5 (in β-NiS structure) to 6 (in α-NiS structure) during the β- to α-phase transition. This β- to α-phase is a toptactic transition, involving breakage and rearrangement of the Ni–S bonds [1]. As the compositional range of the α-phase is wider than that of the β-phase, the equilibrium compositions of the α- and β-phase depend on the direction of the transition either from α- to β-phase or from β- to α-phase. For the transition from β-NiS to α-NiS, all the β-phase transforms into the α-phase with no variations in composition. For the transition from a nickel-deficient α-$Ni_{1-x}S$ to β-NiS, the exsolution of more nickel-rich β-NiS from the nickel-deficient α-$Ni_{1-x}S$ host will make the α-phase host even more deficient in Ni.

The equimolar composition, α-NiS, becomes progressively metal deficient, α-$Ni_{1-x}S$, at high temperatures, accompanied by the exsolution of Ni_3S_2 and/or Ni_7S_6 [1]. However, the onset decomposition temperature of α-NiS has not been precisely determined. The present study attempts to reconcile the ambiguities regarding the stoichiometric effect on the decomposition of the α-phase upon heating and the α- to β-phase transition at ambient pressure.

2. Experimental

2.1 *Synthesis*

Standard silica-tube techniques [15, 16] were adopted to synthesize α-NiS/α-$Ni_{1-x}S$. Precisely weighed Ni (1 mm diameter wire 99.9+%, Aldrich) and S (granules 99.99+%, Aldrich) were sealed under vacuum in 10 mm diameter silica tubes. A series of bulk compositions of

α-NiS/α-$Ni_{1-x}S$ were selected, ranging from NiS, $Ni_{0.97}S$ to $Ni_{0.92}S$. Three heating schedules were adopted to study the decomposition behavior of α-NiS/α-$Ni_{1-x}S$. Details of the trial schedules are listed in table 1. The slow heating schedule and soaking process were employed to minimize tube failure due to high sulfur vapor pressure above 723 K. The tubes were quenched to room temperature in cold water. The charges were removed from the tubes and ground to fine powder under acetone, ensuring the homogeneity of the mss (monosulfide solid solution, $Ni_{1-x}S$). The samples were then resealed in new silica tubes and heated according to the three different schedules, then quenched to produce the metastable phase α-NiS/α-$Ni_{1-x}S$. A series of anneal/quench experiments were performed on the synthesized samples over the temperature range 323 to 643 K for a bulk composition of NiS, from 523 to 613 K for a bulk composition of $Ni_{0.97}S$, and from 523 to 573 K for a bulk composition of $Ni_{0.92}S$, with annealing periods of up to 24 h. The temperature in the muffle furnaces was controlled within an error range of ±5 K.

2.2 *X-Ray diffraction*

Room-temperature X-ray powder diffraction patterns of the quenched products were obtained using a 100 mm diameter *Guinier Hägg* camera with Cr-$K_{\alpha 1}$ radiation ($\lambda = 2.2897$ Å). The finely powdered sample was mixed with a small amount pure Si, which was used as an internal standard. The *Guinier Hägg* films were scanned in *TPU/Pos* mode using an Epson film scanner, and the powder diffraction profiles over 2θ-range 10 to 90° were extracted using the programs *Scion Image* and *Universal-Si-Calibration*, a macro function based on *Igor Pro 4.0*. Weight fractions of various phases were determined by Rietveld refinement [17]. Atom occupancies, profile parameters, cell parameters, overall temperature factor, and phase scale factors were refined. The Rietveld method [18, 19] reveals the detailed structure and composition of a polycrystalline sample [20]. The Pseudo-Voigt function was adopted to model the peak shapes of X-ray diffraction patterns. Refined parameters were: peak shape variables (U, V, W), background (Shifted Cheby I function), scale factor (S), cell parameters ($a, b, c, \alpha, \beta, \gamma$), and thermal displacement (B). Cell and thermal constraints were employed during the Rietveld refinements. The refinement of these parameters integrates each intensity into a properly shaped reflection, which contributes to the overall diffraction pattern. The result is a calculated X-ray diffraction profile that best fits the experimental intensities of X-ray diffraction peak. GOF (goodness of fit) was used to assess the success or otherwise of the refinement procedure, as it integrates the number of observation into the least-squares method.

Quantitative phase analysis was performed on each sample using the formalism described by Hill and Howard [21]. The weight fraction of a phase can be described as:

$$w_{\mathrm{p}} = \frac{(SZMV)_p}{\sum(SZMV)_i} \tag{1}$$

where w_{p} is the weight fraction of phase P, S is the scale factor, Z is the number of formula units per unit cell, M is the molecular weight of the formula unit, and V is the volume of unit cell.

Any variation of the stoichiometry of α-$Ni_{1-x}S$ or β-$Ni_{1-y}S$ over the course of the α- to β-phase transition will be reflected in changes in the cell parameters [1, 8]. Thus, the cell parameters are refined for each phase in the X-ray powder profile. Initial input cell parameters and atom positions for the Rietveld refinement were taken from Vaidya [22] for α-NiS and α-$Ni_{1-x}S$, Metcalf *et al.* [23] for Ni_3S_2, Lundqvist (1947) for Ni_3S_4 [24], and Fleet (1972) for α-Ni_7S_6 [25]. The powder refinement-conformed structure model of β-NiS/β-$Ni_{1-y}S$ in space group $R3m$ proposed by Grice and Ferguson [26] and Rajamani and Prewitt [27] was adopted.

Table 1. Summary of the three trial runs of the treatment schedule for NiS/$Ni_{1-x}S$. All samples were quenched from annealing temperature to 298 K. T_{ann} and t_{ann} are annealing temperature and time respectively. Variations in processing parameters during the "Pre-treatment" for each run are underlined. Possible/uncertain phases (due to low concentrations) are denoted by "?", *e.g.* Ni_3S_2?.

Sche. No.	Raw Mat.	Description of synthesis and treatment			Bulk Comp.	Products
			Anneal-quench			
		Pre-treatment	T_{ann} (K)	t_{ann} (day)		
1	S	▪ Vacuum-seal the raw materials in glass tube →			NiS	α-$Ni_{1-x}S$
	Ni	▪ Heat the glass tube from 298 to 523 K at rate 2 K/min →				Ni_3S_2
		▪ Heat the glass tube from 523 to 573 K at rate 0.4 K/min →				α-Ni_7S_6?
		▪ Hold at 573 K for 12 h →				
		▪ Heat the glass tube from 573 to 773 K at rate <0.1 K/h →			$Ni_{0.97}S$	α-$Ni_{1-x}S$
		▪ Heat the glass tube from 773 to 1073 K at rate 2.5 K/min →				Ni_3S_2?
		▪ Hold at 1073 K for 5 h →	973	7		
		▪ Quench in cold water →				
		▪ Grind the charge into fine powder and re-seal in glass tube in vacuum →			$Ni_{0.92}S$	α-$Ni_{1-x}S$
		▪ Heat from 289 to 1073 K at rate <80 K/h and hold at 1073 for 2 h →				Ni_3S_2?
		▪ Natural cool from 1073 to 973 K → "Anneal-quench" process				
2	S	▪ Vacuum-seal the raw materials in glass tube →			NiS	α-NiS
	Ni	▪ Heat the glass tube from 298 to 523 K at rate 2 K/min →				
		▪ Heat the glass tube from 523 to 573 K at rate 0.4 K/min →				
		▪ Hold at 573 K for 12 h →				
		▪ Heat the glass tube from 573 to 773 K at rate <0.1 K/h →				
		▪ Heat the glass tube from 773 to 1073 K at rate 2.5 K/min →			$Ni_{0.97}S$	α-$Ni_{1-x}S$
		▪ Hold at 1073 K for 5 h →	773	7		
		▪ Quench in cold water →				
		▪ Grind the charge into fine powder and re-seal in glass tube in vacuum →			$Ni_{0.92}S$	α-$Ni_{1-x}S$
		▪ Place the charge in a pre-heated furnace at 773 K → "Anneal-quench" process				
3	S	▪ Vacuum-seal the raw materials in glass tube →			NiS	α-$Ni_{1-x}S$
	Ni	▪ Heat the glass tube from 298 to 523 K at rate 2 K/min →				Ni_3S_2
		▪ Heat the glass tube from 523 to 573 K at rate 0.4 K/min →				
		▪ Hold at 573 K for 12 h →				
		▪ Heat the glass tube from 573 to 773 K at rate <0.1 K/h →			$Ni_{0.97}S$	α-$Ni_{1-x}S$
		▪ Heat the glass tube from 773 to 1073 K at rate 2.5 K/min →	773	7		Sulfur
		▪ Hold at 1073 K for 5 h →			$Ni_{0.92}S$	α-$Ni_{1-x}S$
		▪ Quench in cold water →				Sulfur
		▪ Grind the charge into fine powder and re-seal in glass tube in vacuum →				
		▪ Heat from 289 to 1373 K at rate <80 K/h and hold at 1073 for 2 h →				
		▪ Natural cool from 1373 to 773 K → "Anneal-quench" process				

2.3 *BSE image and chemical analyses*

Back-scattered electron (BSE) image and chemical analyses were carried out using a PHILIPS XL20 scanning electron microscope at Adelaide Microscopy, University of Adelaide. The analyses were undertaken using an accelerating potential of 20 kV and a specimen current of ~20 nA. A natural sphalerite sample was used as an inner standard of the Energy Dispersive X-ray (EDX) chemical analyses.

3. Results and discussion

3.1 *Decomposition of α-NiS/Ni$_{1-x}$S*

α-NiS/Ni$_{1-x}$S is a metastable phase at low temperatures ($T < 652$ K). Therefore, the anneal–quench technique is needed to produce a homogeneous α-NiS/Ni$_{1-x}$S sample at room temperature. The experimental results show that the annealing temperature from which the synthetic α-NiS/Ni$_{1-x}$S samples were quenched is an essential parameter determining the species of final products. The anneal–quench experiments were performed on the bulk compositions NiS, $Ni_{0.97}S$, and $Ni_{0.92}S$ according to three trial schedules: (1) cool from 1073 to 973 K, anneal at 973 K for 7 days, then quench to room temperature, (2) place samples in a pre-heated furnace at 773 K, anneal at 773 K for 7 days, then quench to room temperature, and (3) cool from 1373 to 773 K, anneal at 773 K for 7 days, then quench to room temperature. The details of each run are summarized in table 1.

XRD examinations of the samples treated by schedule (1) confirmed that a small amount of Ni_3S_2 and possiblya trace amount of metastable α-Ni_7S_6 are produced from the initial bulk composition NiS (figure 1a). The ingot produced using this schedule is not homogeneous even following prolonged annealing at 973 K. This result contradicts observations of Trahan *et al.* [28], who reported that the ingot produced was homogeneous under similar conditions. A back-scattered electron image (figure 2a) generated from the polished ingot sample confirmed that phase separation had occurred during the synthesis of α-NiS using schedule (1). The darker area (lower mean atomic number) is the α-$Ni_{1-x}S$ with an average composition of $Ni_{0.981}S$. In addition, Ni_3S_2 was observed along the α-$Ni_{1-x}S$ grain edges (figure 2a).

The circled area in figure 2a is amplified in figure 2b. The atomic percentage of Ni in the brighter area (higher mean atomic number) is 53.4%, very close to the composition of Ni_7S_6 (figure 2b). This may be caused by the decomposition of NiS to a sulfur-rich α-$Ni_{1\text{-}x}S$ and the high-temperature heazlewoodite phase ($Ni_{3-x}S_2$) at high temperatures. However, the high-temperature heazlewoodite phase is not quenchable and instantaneously decomposes to Ni_3S_2 (low-temperature heazlewoodite) and Ni_7S_6 at room temperature [1]. The proposed decomposition routes are illustrated in figure 3, a schematic phase diagram derived from the plot of Kullerud and Yund [1]. Although Kullerud and Yund [1] described the phase relations in the Ni–S system, the exact compositional range of α-$Ni_{1-x}S$ *vs* temperature was not detailed. The exsolution of Ni_3S_2 and a possible phase, Ni_7S_6, during the quenching (from 973 K) is more significant for the bulk composition NiS compared with that from the $Ni_{0.97}S$ and $Ni_{0.92}S$ samples. This result may be a consequence of the compositions $Ni_{0.97}S$ and $Ni_{0.92}S$ being deeply 'buried' inside the nonstoichiometry range of α-$Ni_{1-x}S$ at higher temperatures (figure 3). An alternative hypothesis is that the more nickel-deficient samples exsolve less high-temperature heazlewoodite phase ($Ni_{3-x}S_2$), according to the equation:

$$NiS \longrightarrow Ni_{1-x}S + (Ni_{3-x}S_2) \qquad (2)$$

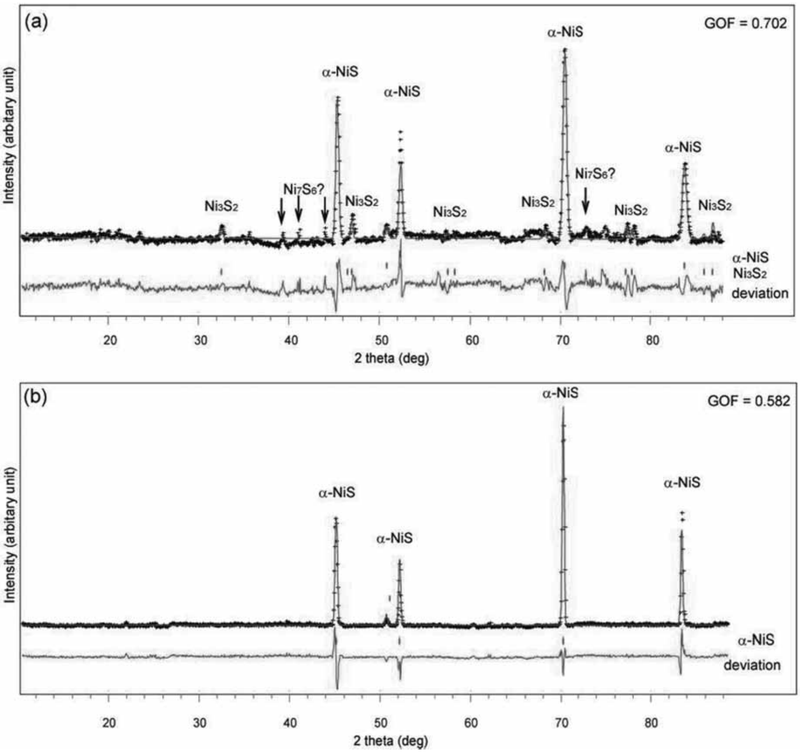

Figure 1. (a) X-ray diffraction patterns ($k_{\alpha,\mathrm{Cr}}$) for the synthetic samples using schedule (1). (b) X-ray diffraction patterns ($k_{\alpha,\mathrm{Cr}}$) obtained using schedule (2).

Samples treated according to schedule (2) yielded almost pure α-NiS/α-Ni$_{1-x}$S (figure 1b). This implies that the annealing temperature (773 K) is below the onset temperature of reaction (2).

3.2 *α- to β-Phase transition for equimolar composition NiS*

The cell and phase data for six sets of isothermal annealing experiments (from 323 to 643 K) on an equimolar composition NiS are summarized in table 2. The cell parameters of the exsolved β-NiS did not change significantly over the course of reaction and the values of the a and c parameters are consistent with those of the equimolar composition β-NiS as reported by Grice and Ferguson [26] but smaller than those reported by Rajamani and Prewitt [27].

The consistency (within error range) of the cell parameters of β-NiS indicates that its composition remains constant over the temperature ranges employed in the current experiments. The cell parameters of α-NiS were more or less constant for five sets of isothermal experiments (annealed at 323, 343, 423, 523, and 643 K) but irregularly fluctuated when annealing at 623 K. Careful inspection of the isothermal data at 633 K shows that this anomalous variation in cell parameter occurred at the end of the reaction, where over 95% of the α-NiS has been transformed into β-NiS. Theses changes are not expected to result from variations in composition of α-NiS according to the mass balance calculation on the assumption of equimolar composition β-NiS. Hence, they may arise from the amplified systematic error of Rietveld refinement for small phase fractions of α-NiS ($<5\%$) [17–19, 21].

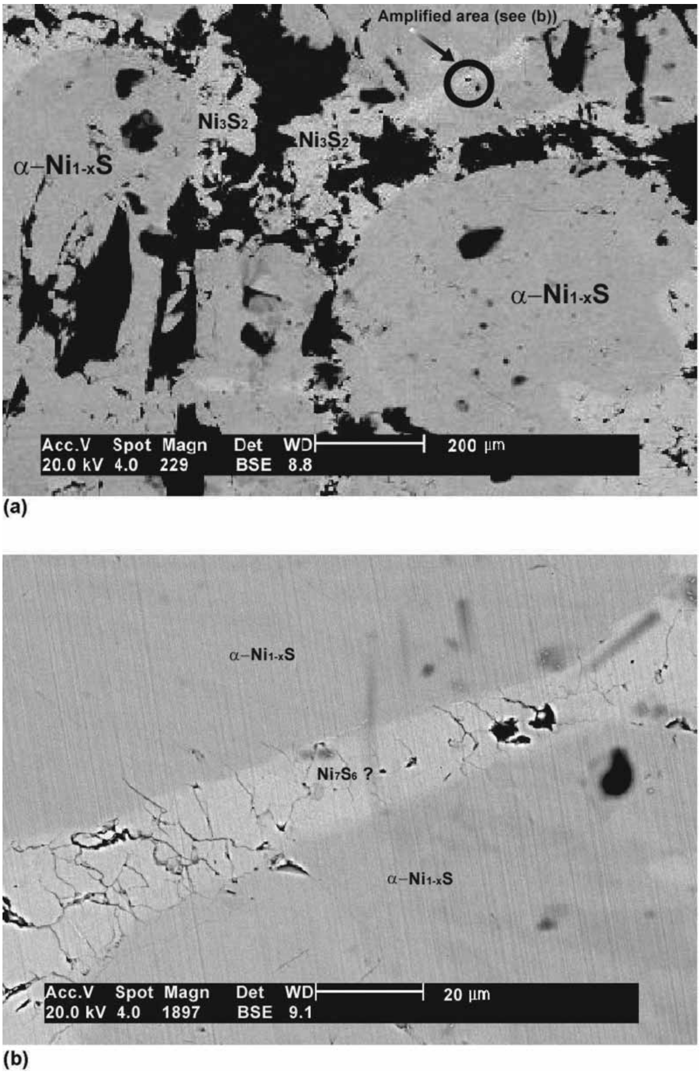

Figure 2. (a) Back-scattered electron image of a polished sample synthesized using schedule 1. The coexistence of α-Ni$_{1-x}$S and Ni$_3$S$_2$ is clear. (b) An enlargement of the circled portion in (a), showing possible minor phase Ni$_7$S$_6$.

Five sets of isothermal data (at 323, 343, 423, 523, and 623 K) were used for the kinetic characterization of the transition α-NiS $\rightarrow$ β-NiS. The α- to β-phase transition kinetics are strongly affected by temperature. The transition rates are relatively rapid. At the highest temperature, 623 K, the reaction was complete within 1 h; in the middle temperature range (423 to 523 K), in 2 to 5 h; and for the lowest temperature, 323 K, in 10 h. The α- to β-phase transition occurs in the temperature range 343–643 K, as there was no β-phase detected outside this range. It is reasonable to believe that below 343 K the transition is very sluggish and so no α- to β-NiS transition could be observed during the time scale of these experiments. Above 643 K, on the other hand, the α-NiS may become the stable phase, therefore no β-NiS would exsolve. According to the results of Kullerud and Yund [1], the onset temperature for β-NiS to transform to α-NiS is 670 K. Therefore, at 643 K ($<$ the onset transition temperature) β-NiS should be the stable phase rather than the α-NiS phase observed in the current study.

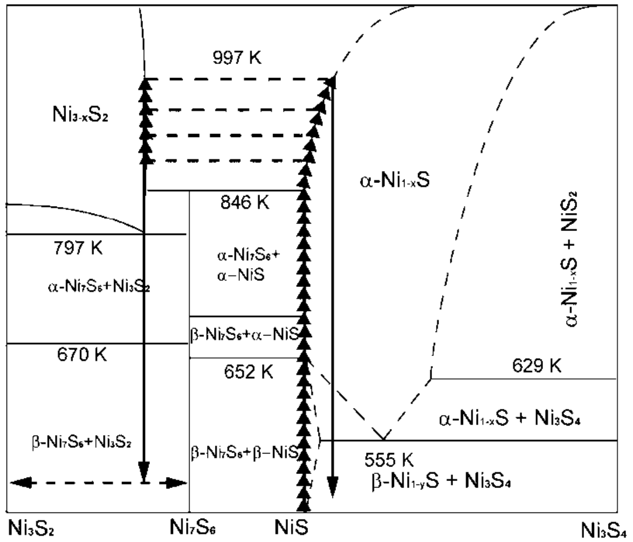

Figure 3. A schematic draft of the partial Ni–S phase diagram, redrawn according to the phase relations in the Ni–S system as described by Kullerud and Yund [1]. The heating and quenching process for an equimolar composition α-NiS is shown. At 997 K, α-NiS decomposes to α-$Ni_{1-x}S$ and higher-temperature heazlewoodite $Ni_{3-x}S_2$. Quenching from 997 K results in the simultaneous decomposition of $Ni_{3-x}S_2$ to Ni_3S_2 and Ni_7S_6. Dashed lines in the phase diagram indicate the compositions of the phases in equilibrium have not been precisely determined.

In order to verify the results of Kullerud and Yund [1], we heated a well-transformed sample (95.2 wt% β-NiS + 4.8 wt% α-NiS) to 673 K (slightly higher than Kullerud and Yund's [1] suggested onset transition temperature of 670 K) and annealed for 24 h. An X-ray diffraction pattern of this annealed sample showed that the β-NiS phase had disappeared and only pure α-NiS remained. The result is consistent with that of Kullerud and Yund [1]. This result also indicates that the reported onset transition temperature of 670 K was derived from a heating process. However, the current annealing experiments should be considered as a 'cooling process' (although restrictively an isothermal process), as the samples were quenched from a temperature (773 K) higher than all the annealing temperatures used in the current isothermal experiments. Thus, the discrepancy in the transition temperature results from the hysteresis effect between heating and cooling processes. According to Hannay [29] most solid-state reactions more or less require a degree of over-heating or -cooling (compared with their thermodynamically determined reaction temperatures) to initiate the reactions, due to kinetic factors. The up-limit temperature for the α- to β-NiS transition in the current study is 623 K (table 2). Hence, the exact transition temperature for α-NiS $\leftrightarrow$ β-NiS lies between 623 K (derived from a 'cooling process' in the current study) and 670 K (derived from a heating process by Kullerud and Yund [1]).

3.3 *α- to β-Phase transition for nickel-deficient compositions $Ni_{1-x}S$*

It has been reported that the sulfur content influences the stability of the high-temperature phase α-$Ni_{1-x}S$, and a eutectoid decomposition of α-$Ni_{1-x}S$ to millerite (β-NiS) and polydymite (Ni_3S_4) has been observed at 555 K [1, 7]. In the current study, nickel-deficient samples, α-$Ni_{1-x}S$, were synthesized to yield two bulk compositions: $Ni_{0.97}S$ and $Ni_{0.92}S$. A series of annealing experiments was performed on these samples in the temperature range 523 to 613 K. The cell and phase data from these experiments are summarized in table 2. At the lowest annealing temperature, 523 K, reasonable amount of Ni_3S_4 exsolved along with the

Table 2. Transitions: α-NiS $\rightarrow$ β-NiS, α-$Ni_{1-x}S$ $\rightarrow$ β-NiS and α-$Ni_{1-x}S$ $\rightarrow$ β-NiS + Ni_3S_4. Summary of results from anneal–quench specimens. α-$Ni_{1-x}S$, β-NiS and Ni_3S_4 in weight percent (wt%); a_α and c_α are cell parameters for α-$Ni_{1-x}S$; a_β and c_β for β-NiS; a_{poly} for Ni_3S_4 (polydymite). Estimated standard deviations are given in parentheses.

Bulk composition	Temp. (K)	Time (h)	Wt % α-NiS	Wt % β-NiS	Wt % Ni_3S_4	a_α (Å)	c_α (Å)	a_β (Å)	c_β (Å)	a_{poly} (Å)
NiS	323	1	99.9(3)			3.4383(6)	5.348(1)			
		5	99.9(4)			3.4383(6)	5.348(1)			
		24	99.9(2)			3.4382(6)	5.348(1)			
	343	1	78.7(6)	21.3(7)		3.4381(7)	5.348(1)	9.607(1)	3.1485(6)	
		2	58.0(7)	42.0(7)		3.4381(7)	5.348(1)	9.607(1)	3.1479(7)	
		4	39.7(6)	60.3(7)		3.4382(7)	5.348(1)	9.606 (1)	3.1482(6)	
		10		99.0(7)				9.606(1)	3.1477(8)	
		24		99.2(7)				9.606(1)	3.1479(6)	
	423	1	46.9(6)	53.1(8)		3.4376(6)	5.347(1)	9.6066(8)	3.1484(6)	
		2	23.0(6)	77.0(7)		3.4382(6)	5.347(1)	9.607(1)	3.1478(7)	
		3	11.1(6)	88.9(8)		3.4380(6)	5.347(1)	9.607(1)	3.1480(7)	
		5		99.5(7)				9.606(1)	3.1474(6)	
		24		99.1(8)				9.6069(7)	3.1481(6)	
	523	0.5	54.9(6)	45.1(7)		3.4383(7)	5.347(1)	9.607(1)	3.1482(6)	
		1	13.0(6)	87.0(7)		3.4383(7)	5.347(1)	9.607(1)	3.1477(8)	
		1.5	3.5(6)	96.5(8)		3.438(1)	5.3477(7)	9.607(1)	3.1476(6)	
		2	1.5(6)	98.5(7)				9.606(1)	3.1481(6)	
		5	1.6(6)	98.4(6)				9.606(1)	3.1481(7)	
	623	0.25	64.8(6)	35.2(6)		3.4381(6)	5.337 (1)	9.607(1)	3.1480(7)	
		0.5	29.0(6)	71.0(7)		3.4382(5)	5.3380(8)	9.607(1)	3.1485(6)	
		1	5.5(6)	94.5(7)		3.4360(9)	5.339(1)	9.607(1)	3.1481(8)	
		1.5	4.7(6)	95.3(8)		3.4372(9)	5.337(1)	9.606(1)	3.1477(6)	
		3	4.8(6)	95.2(7)		3.436(1)	5.339(1)	9.606(1)	3.1484(6)	
	643	1	99.9(6)			3.4384(6)	5.348(1)			
		24	99.9(6)			3.4384(6)	5.348(1)			
$Ni_{0.97}S$	523	1	29.1(7)	65.1(7)	5.8(6)	3.4314(6)	5.332(1)	9.606(1)	3.1485(6)	9.457(1)
		24		90.2(7)	9.7(6)			9.606(1)	3.1484(7)	9.456(1)
	573	1	82.8(7)	17.2(6)		3.4313(6)	5.338(1)	9.607(1)	3.1485(6)	
		1.5	71.1(7)	28.9(7)		3.4316(6)	5.337(1)	9.607(1)	3.1482(6)	
		2	34.0(7)	66.0(6)		3.4230(7)	5.328(1)	9.607(1)	3.1482(6)	
		3	25.0(6)	75.0(7)		3.4211(7)	5.322(1)	9.607(1)	3.1479(5)	
		4	24.3(6)	75.7(6)		3.4219(7)	5.320(1)	9.605(1)	3.1480(6)	
		5	24.3(6)	75.7(6)		3.4216(7)	5.321(1)	9.605(1)	3.1477(5)	
	593	0.5	86.9(7)	13.1(7)		3.4330(6)	5.339(1)	9.607(1)	3.1484(5)	
		1	76.8(7)	23.2(7)		3.4327(6)	5.338(1)	9.607(1)	3.1485(5)	
		1.5	34.7(8)	65.3(6)		3.4228(6)	5.327(1)	9.606(1)	3.1485(5)	
		2	33.0(7)	67.0(6)		3.4226(7)	5.323(1)	9.606(1)	3.1483(6)	
		3	32.2(7)	67.8(6)		3.4221(7)	5.323(1)	9.605(1)	3.1479(5)	
		5	32.1(7)	67.9(7)		3.4220(7)	5.323(1)	9.605(1)	3.1476(6)	
	613	1	99.9(5)			3.4234(8)	5.345(1)			
		3	99.4(6)			3.4239(6)	5.344(1)			
		24	99.7(5)			3.4237(6)	5.345(1)			
$Ni_{0.92}S$	523	1	60.4(7)	35.5(6)	4.1(6)	3.4188(7)	5.320(1)	9.606(1)	3.1482(6)	9.457(1)
		10	8.2(7)	67.3(7)	24.5(7)	3.4220(7)	5.322(1)	9.606(1)	3.1480(6)	9.457(1)
		24		73.2(7)	26.8(6)			9.605(1)	3.1475(6)	9.456(1)
	573	1	99.9(4)			3.4201(7)	5.331(1)			
		10	96.2(5)		3.8(9)	3.4200(7)	5.331(1)			9.457(1)
		24	96.1(5)		3.9(6)	3.4206(7)	5.332(1)			9.456(1)

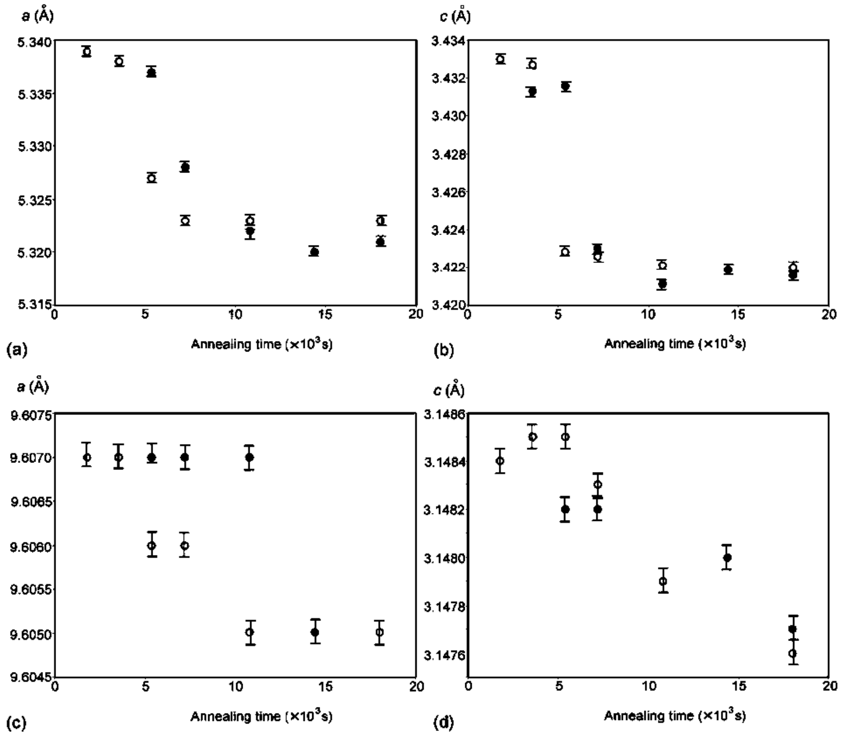

Figure 4. Variations of cell parameters with annealing time for α-$Ni_{1-x}S$ and β-$Ni_{1-y}S$. (a), (b) are a and c parameters of α-$Ni_{1-x}S$ at 573 K (●) and 593 K (○). (c), (d) are a and c parameters of β-$Ni_{1-x}S$ at 573 K (●) and 593 K (○). Initial bulk composition, $Ni_{0.97}S$. Error bars are shown in the figure.

major product β-$Ni_{1-y}S$. There, we use the formula β-$Ni_{1-y}S$ rather than β-NiS (as in the discussions for the equimolar bulk NiS), because the composition of β-nickel monosulfides may have altered slightly over the course of thse reactions, as indicated by the variation in cell parameters. The variations in a and c parameters with annealing time are plotted for both the α- (figure 4a, b) and β-phase (figure 4c, d) at 573 and 593 K.

Noticeably, the c and a parameters of β-nickel monosulfide decreased slightly with progress of the α- to β-phase transition for the initial bulks: $Ni_{0.97}S$ and $Ni_{0.92}S$ (table 2), compared with the relatively constant cell parameters of the β-phase when the initial bulk was NiS (table 2). Table 2 shows that the cell parameters of α-$Ni_{1-x}S$ also decrease over the transition, and vary by larger extents than do the cell parameters of β-$Ni_{1-y}S$. Thus, it is a reasonable assumption that the compositional variation for α-$Ni_{1-x}S$ is more distinct than that for β-$Ni_{1-y}S$ over the course of α- to β-phase transition. This assumption is supported by the results of Kullerud and Yund [1].

Unlike the α-NiS → β-NiS, the transition α-$Ni_{1-x}S \rightarrow \beta$-$Ni_{1-y}S$ might not go to completion, due to the difference in their compositional ranges. This results in a two-phase area in the Ni–S phase diagram, where α and β phases coexist in equilibrium. Attempts have been made to construct the relationship between α-$Ni_{1-x}S$ composition and annealing time. However, for the initial bulk $Ni_{0.97}S$, a composition near to the NiS end, care is required for mathematical calculation of the compositions of α-$Ni_{1-x}S$ and β-$Ni_{1-y}S$. The near-NiS bulk ($Ni_{0.97}S$) can cause significant calculation errors if the composition of the β-phase deviates slightly from NiS. The compositional variation of β-nickel monosulfides is normally negligible, and the β-phase is often expressed in the form of β-NiS, due to its narrow compositional range near NiS [14, 30–33]. For the sample annealed at 573 K for 3 h, for instance, if the β-phase composition changes from NiS to $Ni_{0.99}S$ the calculated composition for the α-phase will change from $Ni_{0.88}S$ to $Ni_{0.91}S$. Additionally, our results show slight variations in the cell parameters for the β-phase, confirming that the hypothesis of varying composition of β-phase is more than likely. Many studies have been performed on phase relations in the Ni–S system, and the relationship between compositional range of β-$Ni_{1-y}S$ and temperature has not been accurately established [1, 30, 34]. In the current study, a more nickel-deficient bulk $Ni_{0.92}S$ was synthesized and isothermal annealings were performed at 523 and 573 K (table 2). The results show that the α- and β-phase do not coexist in equilibrium at both temperatures. At 523 K, β-nickel monosulfide gradually exsolved, along with the formation of small amount of Ni_3S_4. After annealing for 24 h, the α-$Ni_{1-x}S$ disappeared leaving 73.2 wt.% β-nickel monosulfide and 26.8 N_3S_4. At 573 K, no β-nickel monosulfide was observed. The reaction reached equilibrium within 10 h with 3.8 wt.% Ni_3S_4 and 96.2 wt.% α-$Ni_{1-x}S$. The increase in bulk sulfur content narrows the temperature range for coexistence of the α- and β-phase [7]. The bulk composition $Ni_{0.92}S$, however, might have crossed the α- and β- two-phase zone and located to the left of the eutectic composition of α-$Ni_{1-x}S$. α-$Ni_{1-x}S$ coexists with Ni_3S_4 above the eutectic point, 553 K, and below this temperature β-nickel monosulfide is stable in equilibrium with Ni_3S_4 [1].

References

[1] G. Kullerud, R.A. Yund. *J. Petrol.*, **3**, 126 (1962).
[2] W. Haidinger. *Handbuch der bestimmenden Mineralogie, Neue Ausgabe zur Jubelfeier des Verfassers*, Vienna, Austria (1845).
[3] S.R. Krishnakumar, N. Shanthi, D.D. Sarma. *Phys. Rev., Part B*, **66**, 115105 (2002).
[4] G.P. Power. *Aust. J. Chem.*, **34**, 2287 (1981).
[5] R.C. Hubli, T.K. Mukherjee, S. Venkatachalam, R.G. Bautista, C.K. Gupta. *Hydrometallurgy*, **38**, 149 (1995).
[6] D.L. Legrand, H.W. Nesbitt, G.M. Bancroft. *Am. Mineral.*, **83**, 1256 (1998).
[7] F. Grønvold, S. Stølen. *Thermochim. Acta*, **266**, 213 (1995).
[8] S. Stølen, H. Fjellvåg, F. Grønvold, H. Seim, E.F. Westrum. *J. Chem. Thermodyn.*, **26**, 987 (1994).
[9] H. Rau. *J. Phys. Chem. Solids*, **36**, 1199 (1975).
[10] J.T. Sparks, T. Komoto. *J. Appl. Phys.*,**34**, 1191 (1963).
[11] M. Nakamura, A. Sekiyama, H. Namatame, H. Kino, A. Fujimori. *Phys. Rev. Lett.*, **73**, 2891 (1994).
[12] H. Okamura, J. Naitoh, T. Nanba, M. Matoba, M. Nishioka, S. Anzai, I. Shimoyama, K. Fukui, H. Miura, H. Nakagawa, K. Nakagawa, T. Kinoshita. *Solid State Commun.*, **112**, 91 (1999).
[13] H.W. Nesbitt, M. Reinke. *Am. Mineral.*, **84**, 639 (1999).
[14] H. Sowa, H. Ahsbahs, W. Schmitz. *Phys. Chem. Minerals*, **31**, 321 (2004).
[15] G. Kullerud. *Experimental Techniques in Dry Sulfide Research.* In *Research Techniques for High Pressure and High Temperature*, G.C. Ulmer (Ed.), Springer-Verlag, Berlin (1971).
[16] D.J. Vaughan, J.R. Craig. *Mineral Chemistry of Metal Sulfides.* Cambridge University Press, Cambridge (1978).
[17] B.A. Hunter. Rietica 1.7.7., ANSTO, Sydney, Australia (1997).
[18] H.M. Rietveld. *Acta Crystallogr.*, **22**, 151 (1967).
[19] H.M. Rietveld. *J. Appl. Crystallogr.*, **2**, 65 (1969).
[20] E.H. Kisi. *Mater. Forum.*, **18**, 135 (1994).
[21] R.J. Hill, C.J. Howard. *J. Appl. Crystallogr.*, **18**, 173 (1985).
[22] N. Vaidya. *Indian J. Pure Appl. Phys.*, **14**, 600 (1976).
[23] P.A. Metcalf, P. Fanwick, Z. Kakol, J.M. Honig. *J. Solid State Chem.*, **104**, 81 (1993).
[24] D. Lundqvist. *Ark. Kem. Mineral. Geol.*, A**24**, 1 (1947).
[25] M.E. Fleet. *Acta Crystallogr., Sect. B*, **28**, 1237 (1972).
[26] J.D. Grice, R.B. Ferguson. *Can. Mineral.*, **12**, 248 (1974).
[27] V. Rajamani, C.T. Prewitt. *Can. Mineral.*, **12**, 253 (1974)
[28] J. Trahan, R.G. Goodrich, S.F. Watkins. *Phys. Rev., Part B*, **2**, 2895 (1970).
[29] N.B. Hannay. *Solid-state Chemistry*, Englewood Cliffs, New Jersey, USA (1967).
[30] D.B. McWhan, M. Marezio, J.P. Remeika, P.D. Dernier. *Phys. Rev., Part B*, **5**, 2552 (1972).
[31] N. Chen, W. Zhang, Y.O. Yu. *Mat. Lett.*, **55**, 230 (2002).
[32] W. Mulak, P. Balaz, M. Chojnacka. *Int. J. Miner. Process.*, **66**, 233 (2002).
[33] H. Sowa, E. Koch, W. Fischer. *Acta Crystallogr., Sect. A.*, **59**, 317 (2003).
[34] D.D. Sarma, S.R. Krishnakumar, N. Chandrasekharan, E. Weschke C. Schüßler-Langeheine, L. Kilian, G. Kaindl. *Phys. Rev. Lett.*, **80**, 1284 (1998).